

RESEARCH ARTICLE

Small heat shock proteins determine synapse number and neuronal activity during development

Elena Santana¹, Teresa de los Reyes¹, Sergio Casas-Tintó¹ *

Instituto Cajal, CSIC, Madrid, Spain

* These authors contributed equally to this work.

* scasas@cajal.csic.es**OPEN ACCESS**

Citation: Santana E, de los Reyes T, Casas-Tintó S (2020) Small heat shock proteins determine synapse number and neuronal activity during development. PLoS ONE 15(5): e0233231. <https://doi.org/10.1371/journal.pone.0233231>

Editor: Harm H. Kampinga, Universitair Medisch Centrum Groningen, NETHERLANDS

Received: February 18, 2020

Accepted: April 30, 2020

Published: May 21, 2020

Peer Review History: PLOS recognizes the benefits of transparency in the peer review process; therefore, we enable the publication of all of the content of peer review and author responses alongside final, published articles. The editorial history of this article is available here: <https://doi.org/10.1371/journal.pone.0233231>

Copyright: © 2020 Santana et al. This is an open access article distributed under the terms of the [Creative Commons Attribution License](https://creativecommons.org/licenses/by/4.0/), which permits unrestricted use, distribution, and reproduction in any medium, provided the original author and source are credited.

Data Availability Statement: All relevant data are within the paper and its Supporting Information files.

Funding: We would like to declare that this research has been funded by grant BFU2015-

Abstract

Environmental changes cause stress, Reactive Oxygen Species and unfolded protein accumulation which hamper synaptic activity and trigger cell death. Heat shock proteins (HSPs) assist protein refolding to maintain proteostasis and cellular integrity. Mechanisms regulating the activity of HSPs include transcription factors and posttranslational modifications that ensure a rapid response. HSPs preserve synaptic function in the nervous system upon environmental insults or pathological factors and contribute to the coupling between environmental cues and neuron control of development. We have performed a biased screening in *Drosophila melanogaster* searching for synaptogenic modulators among HSPs during development. We explore the role of two small-HSPs (sHSPs), sHSP23 and sHSP26 in synaptogenesis and neuronal activity. Both sHSPs immunoprecipitate together and the equilibrium between both chaperones is required for neuronal development and activity. The molecular mechanism controlling HSP23 and HSP26 accumulation in neurons relies on a novel gene (*CG1561*), which we name *Pinkman* (*pkm*). We propose that sHSPs and Pkm are targets to modulate the impact of stress in neurons and to prevent synapse loss.

Introduction

Synaptic dynamics remodel neuronal circuits under stress conditions [1]. The Heat Shock Protein family (HSPs) is involved in preserving cellular functions such as stress tolerance, protein folding and degradation, cytoskeleton integrity, cell cycle and cell death [2–7]. HSPs are molecular chaperones that represent an intracellular protein quality system to maintain cellular protein homeostasis, preventing aggregation and promoting protein de novo folding or refolding and degradation of misfolded proteins [8]. In addition, HSPs participate in developmental functions in a stress-independent manner [9, 10]. In *Drosophila* development *small Heat Shock proteins* (*sHsps*) have a specific temporal and spatial pattern of expression [10]. In particular, *sHsp23* and *sHsp26* show high expression levels in CNS during development, suggesting a role in neural development [10].

65685P from the Spanish MICINN. The funders had no role in study design, data collection and analysis, decision to publish, or preparation of the manuscript.

Competing interests: The authors have declared that no competing interests exist.

sHSPs include a large group of proteins represented in all kingdoms of life [11], with a conserved protein binding domain of approximately 80 amino-acid alpha crystallin [12]. These molecular chaperones were initially described as low molecular weight chaperones that associate early with misfolded proteins and facilitate refolding or degradation by other chaperones and co-factors [11] [13]. However, members of the sHSPs have diverse functions beyond the chaperon activity including cytoskeleton assembly [14], the suppression of reactive oxygen species, anti-inflammatory, autophagy, anti-apoptotic and developmental functions (reviewed in [2]). sHSPs represent the most extended subfamily of HSPs, albeit the less conserved [15]. sHSPs have a conserved primary structure divided in three elements required for their function: 1) a variable N-terminal long-sequence related to oligomerization, 2) the conserved α -crystallin domain required for dimers formation that represents the main hallmark of sHSPs family, and 3) a flexible short C-terminal sequence mediating oligomers stability [11, 16]. Post-translational modifications in sHSPs shift the folding/degradation balance and, in consequence, alter dimer or oligomer formation and function [11, 17]. This chaperone control system modulates critical decisions for the folding or degradation proteins and a failure causes pathological conditions [17].

HSPs protect synaptic function in the nervous system from environmental insults or pathological factors [18–20] (reviewed in [21]), and are also associated to neurodegenerative diseases, aberrant protein-induced neurotoxicity and disease progression [13]. The sHSPs family is involved as a non-canonical role in *Drosophila* development and other biological processes such as synaptic transmission [22]. However, its implication in synaptic dynamics during development has not been described yet. Synapse number can be altered due to the influence of physiological parameters (aging, hormonal state, exercise) [23–26], pathological (neurodegenerative process) [27, 28] or induced conditions (mutants) [29] which alter cellular components and pathways [30]. The imbalance between the pro- and anti-synaptogenic pathways modulates the number of synapses [30]. The neuromuscular junction (NMJ) of *Drosophila melanogaster* is a stereotyped structure well established for the study of synapses [31]. Most of the molecules involved in synaptic transmission are conserved between *Drosophila* and vertebrates thus, this model system is well established for the study of synapses [32].

Here, we study the contribution of two sHsps, sHp23 and sHsp26 in the development of the CNS and synapse modulation. sHsp23 and sHsp26 are expressed in the CNS during the development [10, 33, 34] but their function remains unclear. In addition, we describe the function of CG1561, named Pinkman (Pkm), as a novel putative kinase that interacts with sHSP23 and sHSP26. Pkm regulates expression and protein stability and participates in the establishment of synapse number during development.

Materials and methods

Drosophila strains

Flies were maintained at 25°C in fly food in cycles of 12 hours of light and 12 hours of darkness. The following stocks were used: *UAS.LacZ* (gift from Dr. Würz). Fly stocks from the Bloomington Stock Center: *Gal4.D42* (BL-8816), *UAS.Hsp23* (BL-30541), *P{UAS-mLex-A-VP16-NFAT}H2/TM3*, *Sb1* (BL- 66543), *P{LexAop-CD8-GFP-2A-CD8-GFP}2*; *P{UAS-mLex-A-VP16-NFAT}H2*, *P{lexAop-rCD2-GFP}3/TM6B*, *Tb1* (BL-66542). Fly Stocks from Vienna Stocks Center: *Hsp26-GFP-V5-Flag* (VDR318685), *UAS.Hsp26RNAi* and *UAS.CG1561RNAi* (VDR106503 KK (1), VDR32634 GD (2) and VDR32635 GD (3)). Fly Stocks from the FlyORF Zurich ORFeome Project: *UAS.Hsp26* (F000796).

***Drosophila* dissection and immunostaining**

Drosophila third instar larvae were dissected in phosphate-buffered saline (PBS) and fixed with PFA 4% in phosphate-buffered saline (PBS). Then, the samples were washed with PBST (PBS with 0.5% Triton X-100) and blocked with 5% bovine serum albumin (BSA) (Sigma) in PBST. We quantified the total number of active zones per NMJ of third instar larvae. We used the binary system Gal4/UAS (Brand & Perrimon, 1993) to drive all genetic manipulations to motor neurons (D42-Gal4). Active zones were visualized using a mouse monoclonal antibody nc82 (1:20, DSHB, IA) which identifies the protein Bruchpilot, a presynaptic element. Neuronal membranes were visualized with rabbit anti-HRP (1:300, Jackson ImmunoResearch, West Grove, PA). Fluorescent secondary antibodies were Alexa 488 (goat anti-mouse, 1:500, Molecular Probes, Eugene, OR) and Alexa 568 (goat anti-rabbit, 1:500, Molecular Probes). Larvae were mounted in Vectashield medium (Vector Labs, Burlingame, CA). Synapse quantifications were obtained from the NMJ *Drosophila* model in muscle fiber 6/7 of the third abdominal segment only to regulate inter-individual data variability.

To localize sHSP23 or sHSP26, third instar larval brain or NMJ were dissected. We use an Hsp26-GFP-V5 fusion construct. sHSP23 was visualized using an anti-Hsp23 (Sigma-Aldrich S 0821) (1:500), and sHSP26 was visualized using anti-V5 (1:50) (Invitrogen 1718556) and anti-GFP mouse (1:50) (Invitrogen A11122). *Drosophila* brains were mounted in Vectashield with DAPI medium (Vector Labs, Burlingame, CA).

Image acquisition

Confocal Images were acquired at 1024x256 resolution as serial optical sections every 1 μm . We used a 63x objective with a Leica Confocal Microscope TCS SP5 II (Mannheim, Germany). We used IMARIS software (Bitplane, Belfast, UK) to determine the number of mature active zones with the 'spot counter' module.

We visualized Hsp23-Hsp26 co-localization and CaLex signal in ventral ganglia cells of third instar larva brains. We acquired brain images at 1024x1024 resolution as serial optical sections every 1 μm at 20x objective. We acquired ventral ganglia cells images at 1024x1024 resolution, 63x objective with magnification of 2.5. We processed the images and analyzed them with LAS-AF (Leica Application Suite software).

Antibody generation

To detect sHsp26 protein in western blot we generated (Abmart) a mouse monoclonal antibody against the sHsp26 peptide sequence: GKENGAPNGKDK MSLSTLLSLVDELQEPRSP IYELGLGLHPHSRYVLPPLGTQQRRSINGCPCASPICPSSPAGQVLAALRREMANRNDIHWPAT AHVKGDFQVCMDVAQFKPSELNVKVVDDSI LVEGKHEERQDDHGHIMRHFVRRYKVPDGYK AEQVVSQLSSDGVLTVSI PKPQAVEDKSKERI IQIQVGP AHLNVKANESEVK **GKENGA** **PNGKDK**

Co-Immunoprecipitation

For biochemical assays, 5–10 adult fly heads were lysed in immunoprecipitation lysis buffer (NaCl 150 mM, 0.1% Tween-20 (Polyoxyethylene sorbitane monolaureate), TBS pH 7.5). We incubated Protein A/G agarose beads overnight at 4°C with 2 μl of the indicated antibody or control IgG (1:100), followed by incubation at 4°C for 1 h with supernatants. We washed the beads and resuspended in 1 \times SDS-PAGE loading buffer for western blot analysis in a 4%–12% gradient SDS-PAGE for the detection of sHSP23 and sHSP26. After electro-blotted onto nitrocellulose 0.45 μM (GE Healthcare) 100V for 1 hour, we blocked the membranes in

TBS-Tween-20 buffer with 5% BSA. We incubated the membranes overnight at 4°C in constant agitation with anti-Hsp23 antibody (1:1000) (Sigma-Aldrich S0821), anti-Hsp26 (1:1000) (Abmart) We visualized the antibody-protein interaction by chemoluminescence using IRDye Secondary Antibodies anti-mouse (IRDye 800CW, LI-COR), anti-rabbit (IRDye 680 RD, LI-COR) and developed with Odyssey equipment. We used three RNAi tools to downregulate *pkm* expression to replicate this condition. *pkm* RNAi 2 was selected to do the rest of experiments due to the evidences we obtained in the blot assay.

Western blot

5–10 head samples were treated with lysis buffer (TBS1x, 150mMNaCl, IP 50x) and then homogenized and centrifuged 13500 rpm for 5 minutes. After selecting the supernatant we added NuPage 4x (Invitrogen by Thermo Fisher Scientific) and β -mercaptoethanol 5%. Western blot analysis samples were run in a 4%–12% gradient SDS-PAGE for the detection of sHSP23 and sHSP26. After electro-blotted onto nitrocellulose 0.45 μ M (GE Healthcare) 100V for 1 hour, we blocked the membranes in TBS-Tween-20 buffer with 5% BSA. We incubated the membranes overnight at 4°C in constant agitation with anti-Hsp23 antibody (1:1000) (Sigma-Aldrich S0821), anti-Hsp26 (1:1000) (Abmart) We visualized the antibody-protein interaction by chemo luminescence using IRDye Secondary Antibodies anti-mouse (IRDye 800CW, LI-COR), anti-rabbit (IRDye 680 RD, LI-COR) and developed with Odyssey equipment. Tubulin were used as a control.

Gene expression analysis with qPCR

10–15 head tissue samples were treated and homogenized with Trizol (Ambiend for Life technologies). Chloroform was added and then centrifuged 13000 rpm at 4°C for 15 minutes. After discarding the supernatant, the RNA was treated with Isopropanol and then centrifuged 13000 rpm at 4°C for 10 minutes and washed with 75% Ethanol. RNA pellet was dissolved in DNAase RNAase free water. Then we performed a transcriptase reaction and a qPCR assay using *Rp49* gene as a control. Primers for *sHsp23*, *sHsp26*, *Pinkman* and *Cat* were used: *sHsp23* Fv (5'-3') TGCCCTTCTATGAGCCCTAC, *sHsp23* Rv (3'-5') TCCTTTCGGATTTTCGACAC, *sHsp26* Fv (5'-3') TAGCCATCGGGAACCTTGTA, *sHsp26* Rv (3'-5') GTGGACGACTCCATCT TGGT, *pkm* Fv (5'-3') TCGTGCTGGAGGATCTGTCTT, *pkm* Rv (3'-5') CCCGGCCAATGATATAGCAT, *Catalase* Fv (5'-3') TTCGATGTCACCAAGGTCTG, *Catalase* Rv (3'-5') TGCTCCACCTCAGCAAAGTA, *rp49* Fv (5'-3') CCATACAGGCCCAAGATCGT, *rp49* Rv (5'-3') AACCGATGTTGGGCATCAGA.

Statistics

To analyze the data, we used GraphPad Prism 6 GraphPad Software, La Jolla, CA). Data are shown as mean \pm SD. Statistical significance was calculated using D'Agostino & Pearson normality test and a Student's two-tailed t-test with Welch-correction. In case data were not normal, we performed a Student's two-tailed t-test with Mann-Whitney-U correction. For multiple comparisons, we used One-way ANOVA test with Bonferroni post-test. *p value \leq .05; ** p value \leq .01; *** p value \leq .001; **** p value $<$ 0,0001. p value $>$.05 were not considered significant.

Technical considerations

Each experiment condition has its own control sample to reduce external variables.

Results

Heat shock proteins modify synapses in CNS

To determine the effect of HSPs in synaptogenesis, we used the UAS/Gal4 *Drosophila* binary expression system [35] to modify *Hsps* expression in motor neurons using *D42-Gal4* lines. We used UAS-RNAi lines knockdown *sHsp20*, *sHsp22*, *sHsp23*, *sHsp26*, *sHsp27*, *sHsp40*, *Hsp67 Ba*, *sHsp27 Bc*, *Hsp70 Aa*, *Hsp70 Ba* and *Hsp90* (Fig 1A). To visualize the number of active zones in the NMJs we used anti-bruchpilot (brp) antibody. The quantification of the active zones revealed that the knockdown of *sHsp20*, *sHsp22*, *sHsp26*, *sHsp27*, *sHsp40* and *Hsp90* during development provoked a reduction in synapse number. In addition, we tested the effect in synapse number of *sHsp23*, *sHsp26* and *Hsp70* overexpression (Fig 1B). The results show that the upregulation of *sHsp23*, *sHsp26* or *Hsp70* decrease the number of active zones (Fig 1B).

We focused on the role of two sHSPs, sHSP23 and sHSP26, due to their potential role as non-canonical-sHSPs in the CNS and their unexplored implication in synapses modulation. The upregulation of *sHsp23* in presynaptic neurons causes a reduction in synapse number (Fig 1B). In addition, *sHsp26* knockdown or upregulation induces a reduction in synapse number (Fig 1A and Fig 1B). Thus, the results suggest that sHSP23 is not required for synapse formation but in excess it is detrimental for the neuron and causes a reduction of synapse number during development. Besides, modification in any direction of *sHsp26* expression affects to the correct establishment of synapse number during development, suggesting that sHSP26 fine control is required during development for synapse organization.

According to the interactome (flybase) both chaperones are predicted to physically interact with each other [36] (Fig 1C and Fig 1D). Furthermore, sHSP23 and sHSP26, both interact with: CG11534, CG43755 and Pkm (CG1561) proteins [36] (Fig 1C and Fig 1D).

sHSP23 and sHSP26 colocalize in neurons and interact physically

To determine the expression and subcellular localization of sHSP23 and sHSP26 proteins in larval brain we used a green fluorescent reporter tagged form of sHSP26 (HSP26-GFP-V5) and we generated a monoclonal specific antibody against sHSP26 (S1 Fig). We dissected third instar larvae brain and visualized both sHSPs. The data show that sHSP23 and sHSP26 localize in the cytoplasm of CNS cells, in particular in the optic lobes and the central nerve cord (Fig 2A and 2B'). The co-localization of both proteins occurs in neuroblasts and also in ganglion mother cells and differentiated neurons, compatible with a general role in nervous system development.

To further analyze the presence and co-localization of sHSP23 and sHSP26 we analyzed larvae NMJs (Fig 2C–2F'). The confocal images show an accumulation and colocalization of sHSP23 and sHSP26 throughout the NMJ but particularly intense in the synaptic buttons (Fig 2C–2F'). This observation is compatible with a role in synaptic activity as most of the active zones are in the synaptic buttons.

sHSP23 and sHSP26 interact physically

In general, sHSPs proteins exhibit regions susceptible of posttranslational modifications (PTMs) which favor their oligomerization and alter the affinity of interaction by co-chaperones [17, 37]. Since, this mechanism maintains the activity of sHSPs it has been proposed that it regulates their function [17].

The results show that both proteins are localized in the same sub cellular compartments. To determine if both chaperones interact physically, we performed a co-immunoprecipitation assay. We used head protein extracts that were incubated with specific antibodies to

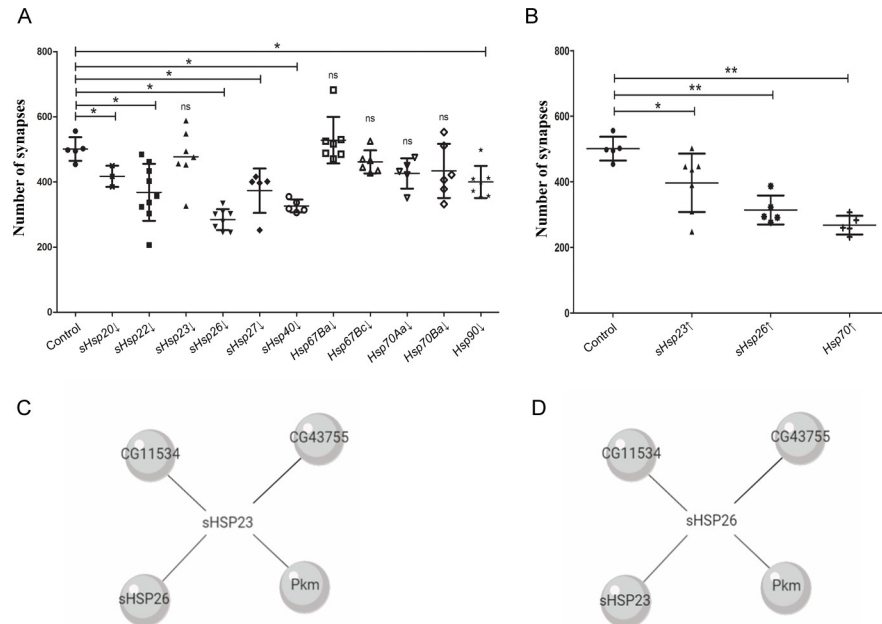


Fig 1. Small heat shock proteins modulate synapses during *Drosophila* development. Synapses quantification screening with *sHsps* genetic tools under *D42* driver expression. (A) Synapses modulation were detected by *sHsp20* RNAi (*sHsp20*↓), *sHsp22* RNAi (*sHsp22*↓), *sHsp23* (*sHsp23*↓), *sHsp26* RNAi (*Hsp26*↓), *sHsp27* RNAi (*Hsp27*↓), *Hsp40* RNAi (*Hsp40*↓), *Hsp90* RNAi (*Hsp90*↓), (B) *UAS.sHsp23* (*Hsp23*↑) *UAS.sHsp26* (*Hsp26*↑) and *UAS.Hsp70* (*Hsp70*↑) samples. One-way ANOVA test with Dunn's multiple comparisons post-test. *p value ≤ .05; ** p value ≤ .01; *** p value ≤ .001. p value > .05 were not considered significant. Error bars show S.D. (C) Diagram of *sHsp23* interactome and (D) diagram of *sHsp26* interactome form <http://flybi.hms.harvard.edu/results.php>.

<https://doi.org/10.1371/journal.pone.0233231.g001>

specifically immobilize each sHSP in Protein A/G agarose beads. Samples were pre-cleared with untagged beads to avoid unspecified binding. Agarose beads were incubated with HSP23 or HSP26 antibody overnight. Head extract proteins and antibody-bound beads were incubated 1 hour. We revealed the western blot membranes with sHSPs antibodies and the results show that sHSP23 (Fig 2G lane 2) immunoprecipitation also precipitates HSP26, and vice versa (Fig 2G lane 3). Both specific bands are corroborated in the input positive control (Fig 2G lane 1) and the lack of signal in the negative control (Fig 2G lane 4) 22c10 antibody). These results confirm the physical interaction between sHSP23 and sHSP26 (Fig 2H), and it is consistent with their co-localization in the motor neuron buttons.

Pkm interacts with sHSP23 and sHSP26 and modulate synapse number

CG11534, CG43755 and Pkm proteins have been postulated that interact with both sHSP23 and sHSP26 (Flybase). They have unknown functions but predicted to have protein kinase like activity (Flybase, <http://flybi.hms.harvard.edu/results.php>). HSPs posttranslational modifications modulate their function [17] and therefore, we quantified the number of active zones in the NMJ upon knockdown of each candidate gene. The knockdown of *pkm* in motor neurons increases synapses number while we could not find any significant change for *CG11534* and *CG43755* knockdown (Fig 3A). In consequence, we focused our study in *pkm* as a candidate gene to interact with *sHsp23* and *sHsp26* in nervous system development.

pkm is a novel gene that encodes a protein with kinase like domains (Flybase) (Fig 3B). Pkm is reported to physically interact with sHSP23 and sHSP26 [36] (Fig 3C). Posttranslational changes modulate chaperones and co-chaperones interaction and activity [17], thus it is

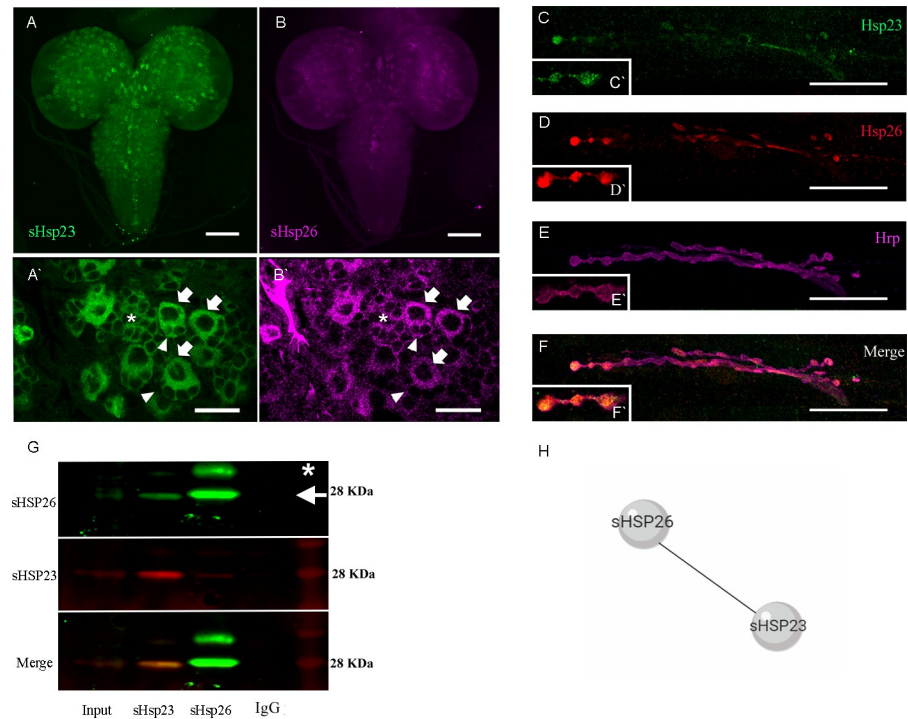


Fig 2. sHSP23 and sHSP26 colocalize in CNS. (A-F) Confocal microscopy images of 3rd instar *Drosophila* larval brain and NMJs. (A) sHSP23 is labeled with anti-GFP antibody driven by *D42-Gal4* to visualize its expression in brain regions (magenta). Scale bar size 100 μ m. (B) sHSP26 is stained with anti-sHSP23 (green). (A'-B') Magnification images of larval brain. Arrows indicate neuroblast, arrowheads indicate ganglion mother cells and asterisk indicate neurons where sHSP23 and sHSP26 colocalize in the cytoplasm. Scale bar size 100 μ m. (C-F) sHSP26 is labeled with anti-GFP antibody driven by *D42-Gal4* to visualize its expression in NMJ (red), sHSP23 is stained with anti-sHSP23 (green) and neuronal membrane is detected with anti-HRP staining (magenta). Scale bar size 50 μ m (C'-F') Magnification images of synaptic boutons in NMJ. (G) Co-Immunoprecipitation assay membrane revealed with sHSP26 (green, arrow) and sHSP23 (red) antibodies in control samples. Fly heads were lysed in immunoprecipitation lysis buffer and incubated with protein A/G agarose beads previously treated with sHSP23 or sHSP26 antibody and IgG antibody as a control. The samples were prepared for western blot analysis. The antibody-protein interaction is visualized by chemoluminescence. Molecular weights are indicated in all the membrane images. * Unknown/unspecific band (H) sHSP23 and sHSP26 interaction diagram.

<https://doi.org/10.1371/journal.pone.0233231.g002>

suggested that these mechanisms represent a system to modulate chaperone dynamics. Accordingly, we did immunoprecipitation assays to determine if *Pkm* was necessary for the sHSP23 and sHSP26 complex formation (Fig 3D). The results revealed that *pkm* knockdown does not modify the interaction between chaperones, thus *pkm* expression is dispensable for sHSP23-sHSP26 physical interaction.

Furthermore, we tested if the expression of *pkm* could modulate the expression of *sHsps*. To evaluate transcription, we did quantitative PCR (qPCR) experiments of *pkm*, *sHsp23*, *sHsp26* and *catalase* (*Cat*) as a positive control. The results show that *pkm* RNAi proved effective since its transcription is drastically reduced (Fig 4A). On the other hand, *sHsp23*, but not *sHsp26*, expression is largely increased (Fig 4A). In order to confirm the transcriptional results, we analyzed the total protein amount of sHSPs upon *pkm* knockdown and those of sHSP23 and sHSP26 by Western blot assays (Fig 4B). To silence the expression of *pkm* we used three RNAi tools to replicate this condition and to reaffirm the regulation changes that we found with the qPCR. The knockdown of *pkm* with *pkm* RNAi 2 tool provokes an increase in sHSP23 and sHSP26 proteins (Fig 4C). The data for *sHsp23* are consistent with the qPCR assays and suggest that *pkm* is necessary to restrict *sHsp23* expression, while *sHsp26* expression is

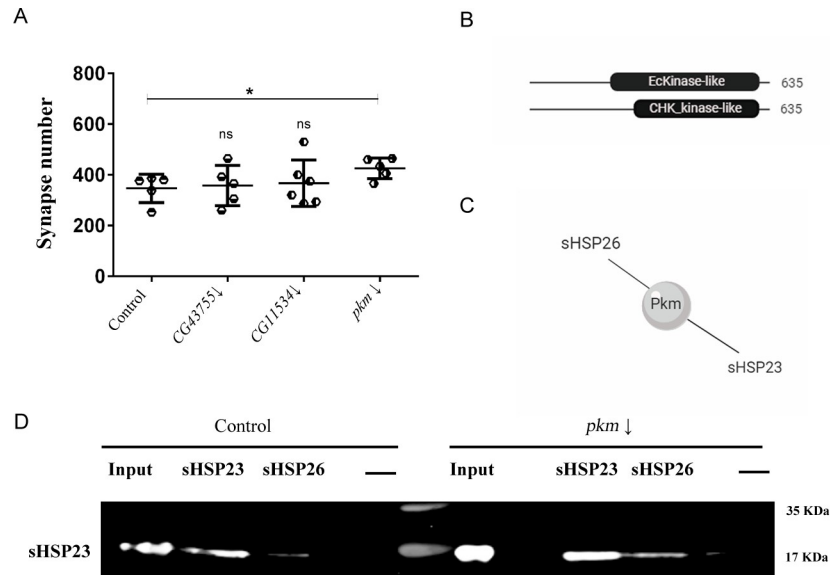


Fig 3. Pkm does not affect sHSP23-sHSP26 interaction. (A) Quantification of synapse active zones in the NMJ is shown for the knockdown of all candidate genes genotypes: *CG43755* RNAi (*CG43755*Δ), *CG11534* RNAi (*CG11534*Δ) and *pkm* RNAi (*pkm*Δ). One-way ANOVA test with Bonferroni post-test* $P < 0.05$. Error bars show S.D. (B) *pkm* contains a EcKinase like (Ecdysteroid kinase-like) domain between 257–545 aa sequence and a CHK_kinase like (Choline kinase-like) domain between 346–543 aa sequence. (C) Diagram of Pkm interactome. Pkm physically interacts with sHSP23 and sHSP26. (D) Co-immunoprecipitation assay membrane revealed with sHSP23 antibody in control and *pkm* RNAi samples. Molecular weights are indicated.

<https://doi.org/10.1371/journal.pone.0233231.g003>

independent of *pkm* expression but protein accumulations is increased upon *pkm* knockdown. These data are compatible with sHSP26 posttranslational modifications mediated by Pkm to control protein stability and degradation.

Pkm modulates synapse number

Small chaperones work as dimers or oligomers to modulate their activity [38], therefore sHSPs protein-protein interaction opens a potential activity as a complex. Since sHSPs family is characterized by forming oligomer assemblies based on dimers joined [39], we investigated the coordinated effect of sHSPs and Pkm.

pkm RNAi causes an increase of synapse number in development (Figs 3A, 4D and 4E), moreover *sHsp23* upregulation reduces synapse number and knockdown does not change synapse number during development (Fig 1). We combined *pkm* RNAi and *sHsp23* upregulation in neurons and we observed an increase in synapse number sample comparable to *pkm* RNAi alone, suggesting that the effect of *pkm* RNAi for synaptogenesis during development is mediated by sHSPs (Fig 4D). These results suggest that the synaptogenic effect of *pkm* knockdown is not restricted to *sHsp23* upregulation (Fig 4A–4C), thus we investigated the contribution of *sHsp26* in combination with *pkm*. Protein quantification experiments show that sHSP26 is accumulated upon *pkm* RNAi expression but in a lesser extent than sHSP23. To demonstrate that sHSP26 is the limiting factor in sHSP23/26 complex we upregulated *sHsp26* together with *pkm* RNAi. Synapse quantifications show that upregulation of *sHsp26* can further increase synapse number in *pkm* RNAi background (Fig 4E). These results suggest that sHSP26 is a limiting factor for synaptogenesis in development and *pkm* reduction contributes to stabilize sHSP26 partially but *sHsp26* upregulation causes complementary synaptogenesis.

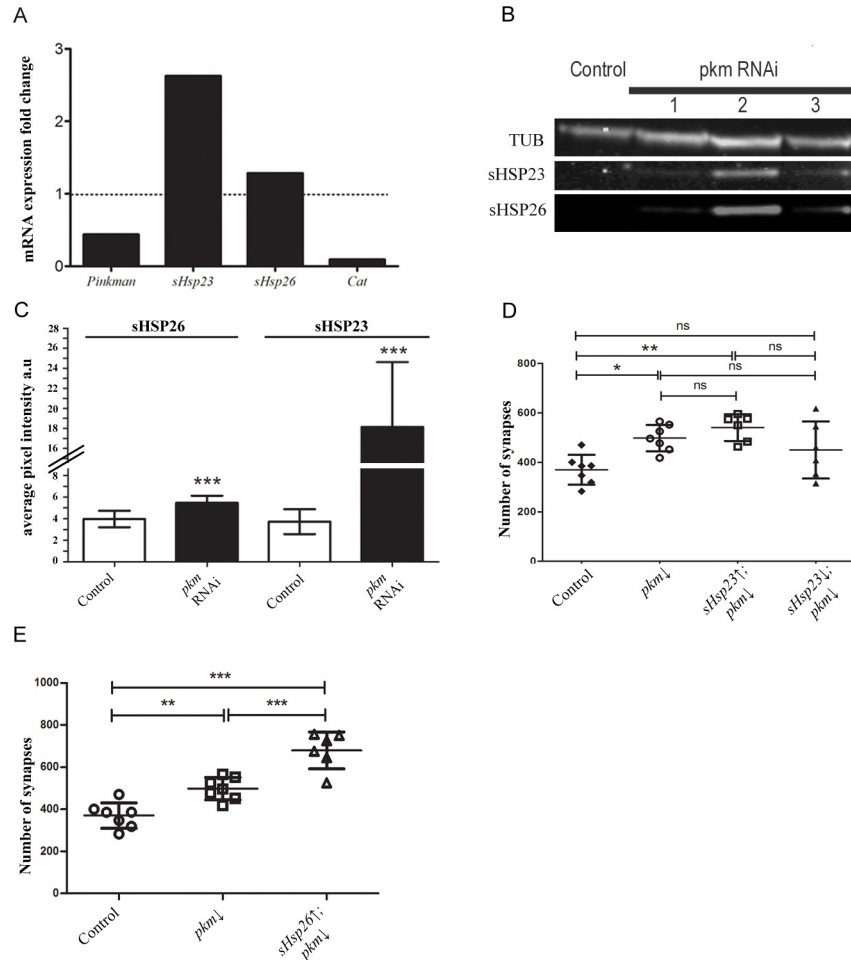


Fig 4. sHSPs amount is regulated by the novel candidate gene *pkm*. (A) qPCR assay of *pkm* RNAi sample measuring mRNA expression fold change of 3rd instar larval of *pkm*, *sHsp23*, *sHsp26* expression and *Cat* as positive control, normalized with *Rp49* as a control. (B) Western blot assay of control and *pkm* RNAi (*pkm*Δ) samples stained against sHSP23 and sHSP26. We used three RNAi tools to confirm the protein amount changes under *pkm* downregulation condition. *pkm* RNAi 2 was selected due to its efficacy. Tubulin was used as a control. (C) Mean Intensity sHSP23 and sHSP26 signal are shown for control and *pkm* RNAi (*pkm*Δ) samples. Unpaired T-test Welch’s correction* P<0.05. Error bars show S.D. (D) Quantification of synapse active zones in the NMJ is shown for the combination of *sHsp23* and *pkm*, *sHsp26* downregulation under *D42* driver expression. (E) Synapse number quantification in NMJs after *sHsp26* upregulation and *pkm* downregulation. Unpaired T-test Mann Whitney post-test * p value<0.05; p value > .05 were not considered significant. Error bars show S.D.

<https://doi.org/10.1371/journal.pone.0233231.g004>

To further determine if sHSPs protein interaction and *pkm* modulation contribute to synaptogenesis, we altered *sHsps* expression together and counted synapse number in NMJs. The joint upregulation of *sHsp23* and 26 induces an increase in synapse number (Fig 5A). This increase contrasts with the reduction elicited by each *sHsp* when upregulated separately (compare to Fig 1A). Moreover, the upregulation of both chaperones in combination with *pkm* knockdown maintains the drastic increase in synapse number and, actually, is of a larger magnitude than the *pkm* knockdown by itself (Fig 5A). This observation is compatible with a functional interaction of Pkm kinase with at least one of the two sHSP analyzed here.

Finally, the combined knockdown of both *sHsps* does not alter synapse number. This result suggests that only the modulation of one single chaperone of this combo produces an imbalance that triggers synapse loss. If both chaperones are reduced in combination, there is no

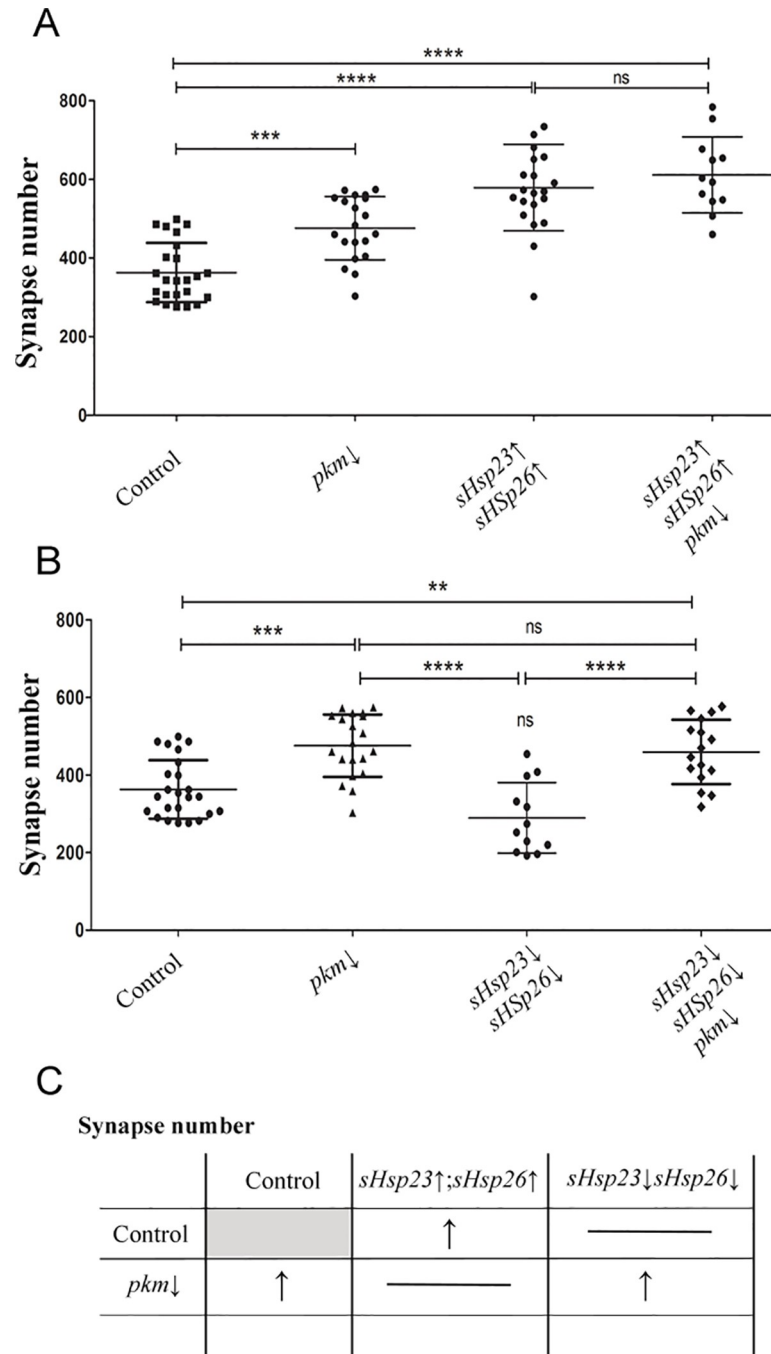


Fig 5. Pkm activity is restricted by sHsps expression. Quantification of synapse active zones in the NMJ is shown for the combination of sHsps expression and *pkm* downregulation under *D42* driver expression: (A) *pkm* RNAi (*pkm*↓), *UAS.sHsp23*; *UAS.sHsps26* (*sHsp23*↑; *sHsp26*↑), *UAS.sHsp23*; *UAS.sHsps26/pkm* RNAi (*sHsp23*↑; *sHsp26*↑/*pkm*↓), (B) *UAS.sHsp23* RNAi; *UAS.sHsps26* RNAi (*sHsp23*↓; *sHsp26*↓), *UAS.sHsp23* RNAi; *UAS.sHsps26* RNAi/*pkm* RNAi (*sHsp23*↓; *sHsp26*↓/*pkm*↓). One-way ANOVA test with Bonferroni post-test. *p value ≤ .05; ** p value ≤ .01; *** p value ≤ .001. p value > .05 were not considered significant. Error bars show S.D. (C) Summary table for the combination of sHsps expression and *pkm* downregulation.

<https://doi.org/10.1371/journal.pone.0233231.g005>

effect what supports the idea that the equilibrium between sHSP23 and sHSP26 is relevant. Moreover, *sHsp23*, *sHsp26* and *pkm* RNAi co-expression show an increase in synapse number

(Fig 5B). Thus, we conclude that the effect of *sHsps* upregulation surpasses *Pkm* contribution but, *sHsps* knockdown is not sufficient to prevent the increase in synapse number caused by *pkm* knockdown (Fig 5B).

As a result, we suggest that sHSP23 and sHSP26 together form a complex that promotes synapse formation in presynaptic neurons, *Pkm* is an anti-synaptogenic element in neurons through, but not restricted to, the modulation of *sHsp23* and *sHsp26* (Fig 5C).

Neuronal activity correlates with synapses changes caused by sHSPs and *Pkm*

Changes in synapse number are expected to reflect on neuronal activity. To evaluate the cellular effect of the observed synapse number changes, we took advantage of CalnexA system (Calcium-dependent nuclear import of *LexA*) to perform a functional assay in motor neurons [40].

CalnexA is a tracing system to label neuronal activity based on calcium/NFAT signaling and the two binary expression systems *UAS/Gal4* and *LexA/LexAop* [41]. We used specific lines to drive a modified NFAT form to motor neurons (*D42.Gal4* and *P{LexAop-CD8-GFP-2A-CD8-GFP}2*; *P{UAS-mLexA-VP16-NFAT}H2*, *P{lexAop-rCD2-GFP}3/TM6B, Tb1*). The accumulation of Ca^{2+} due to the action potentials activates calcineurin which dephosphorylates NFAT, provoking its import into the nucleus. NFAT binds to *LexAop* sequence and induces the expression of a *GFP* reporter gene (Fig 6A). Therefore, *GFP* signal becomes a reporter of neuronal activity.

To evaluate neuronal activity and *sHsps* and *pkm* expression we measured the signal of the *GFP* reporter in larva brains (Fig 6B–6E). The *sHsp23* and *sHsp26* upregulation increases *GFP* signal in cells of ventral nerve cord (Fig 6C and 6E) which correlates with an increase in the number of synapses (Fig 5A). By contrast, *pkm* knockdown reduces CalnexA reporter signal in motor neurons (Fig 6D and 6E) which correlates with its anti-synaptogenic role in motor neurons. The results indicate that *Pkm* contribution is not limited to sHSP23 and sHSP26. Here *pkm* knockdown reproduces the effect of small chaperones upregulation on neuronal activity. Besides, we have shown that *pkm RNAi* synaptogenic effect is not prevented by *sHsp23* and *sHsp26 RNAi* (Fig 5B). Therefore, additional *Pkm* targets participate in synapse formation and neural activity. Taking all these data together, we conclude that *sHsps* and *pkm* expression participate in synapse formation during development and neuronal activity.

Discussion

Synapse regulation is a central event during nervous system development and adult life. Disruptions in the establishment of synapses is associated with morphological, cognitive and psychiatric disorders, but the precise mechanisms underlying these disorders remain unknown [42]. Changes in synapse structure and function are related to paralysis and muscular atrophy in amyotrophic lateral sclerosis (ALS) [43, 44], impairment of the neuromuscular junction function and therefore, motor decline [45] or social and cognitive behaviors related to autism [46]. Thus the study of relevant mechanisms for synapse formation during development is a need.

Chaperones participate in protein folding maintenance as a mechanism to regulate function and pathological conditions, but the specific contribution to synapse number during development was not addressed. Here we describe the combined contribution of two sHSPs (sHSP23 and sHSP26) to synapse formation and the modulation by a novel putative kinase protein *Pkm*. *sHsp23* mRNA and total protein amount increases upon *pkm* knockdown, suggesting a transcriptional negative regulation by *Pkm*.

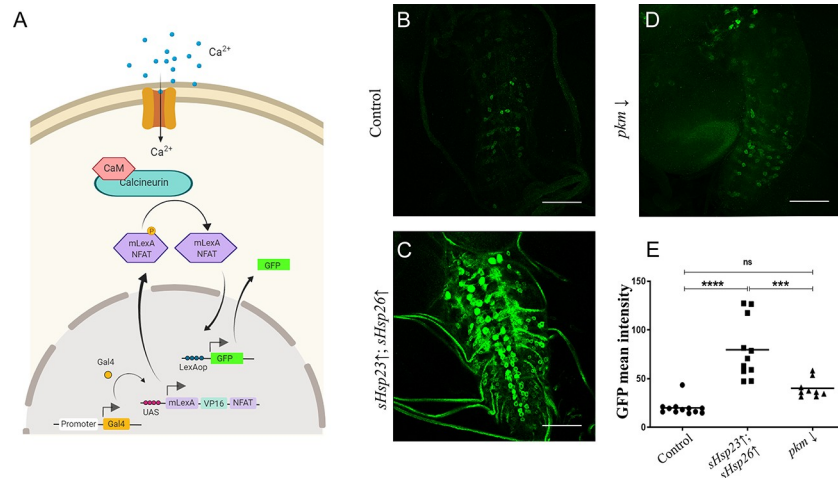


Fig 6. sHSPs contribute to neuronal activity GFP signal. (A) CaLexA system labels neuronal activity based on calcium/NFAT signaling after a neuronal action potential and the two binary expression systems *UAS/Gal4* and *LexA/LexAop*. The accumulation of calcium activates calcineurin that dephosphorylates NFAT that are imported to the nucleus. NFAT binds to LexAop sequence and induces the expression of *GFP* reporter gene that correlates with neuronal activity. (B-D) Confocal microscopy images of 3rd instar *Drosophila* larval ventral nerve cord of (B) control, (C) *UAS.sHsp23; UAS.sHsps26* (*sHsp23*↑; *sHsp26*↑), (D) *pkm* RNAi (*pkm*↓) samples. (E) *GFP* mean intensity signal quantification is shown for *sHsps* expression and *pkm* downregulation under *D42* driver expression: *UAS.sHsp23; UAS.sHsps26* (*sHsp23*↑; *sHsp26*↑), *pkm* RNAi (*pkm*↓), One-way ANOVA test with Bonferroni post-test; *** p value = 0.002. **** p value < 0.0001; p value > .05 were not considered significant. Error bars show S.D.

<https://doi.org/10.1371/journal.pone.0233231.g006>

The results show that *sHsp26* mRNA levels do not show significant changes after *pkm* expression interference. However, *HSP26* in yeast is degraded via a ubiquitin/proteasome-dependent mechanisms [47], the results from western blot experiments show *HSP26* protein accumulation upon *pkm RNAi* expression. Therefore, as *Pkm* is proposed to be a kinase, we cannot discard that *Pkm* could promote *HSP26* post-transcriptional modifications (phosphorylation) to promote its degradation. According to the putative domains present in *Pkm* protein, there are no DNA binding domains and hence it is unlikely that *Pkm* acts as a transcription factor. We postulate that the transcriptional regulation of *sHsp23* is determined by transcription factors sensible to posttranslational modifications as direct targets of *Pkm*. However, the precise mechanisms and molecular details of *Pkm*-*sHSPs* relation require be further investigated.

Genetic modifications of one single *sHsp* (*sHsp23* or *sHsp26*) cause an imbalance in the equilibrium between both genes, as a consequence it causes a reduction in the number of synapses. These results suggest that single alterations in *sHSPs* are detrimental for the number of synapses. However, we propose that *sHSP23* function in synaptogenesis requires forming a complex with *sHSP26*. *sHsp26* upregulation and downregulation modify synapse number in the same direction (synapse number reduction). However, *sHSP23* is the one modulated by *Pkm* but *sHsp23* downregulation does not change synapse number. It is tempting to speculate that a reduction in *sHSP23* does not affect to CNS development and it has a protective function more than synaptogenic. However, when *sHSP23* and *sHSP26* play together they modulate synapses, upregulation of both genes cause an increase in synapse number. Moreover, *pkm* knockdown increases synapse number but does not further increase synapse number upon *sHsps* overexpression, indicating that *pkm* effect on synapses is mediated by *sHsps* regulation. In addition, the combined silencing of *sHsps* does not alter synapse number, in line with the proposal of *sHSPs* equilibrium. But *pkm* knockdown increases significantly the number of synapses in *sHsps* knockdown background. These results suggest that *pkm* is a repressor of *sHsps*

and *pkm RNAi* counteracts the reduction of sHSPs. Thus we speculate with the hypothesis of sHSP26 acting as a synapse modulator and sHSP23 as a protective partner regulated by Pkm.

A direct consequence of *sHsps* modulation is a reduction in neuronal intracellular calcium levels in the brain, an indicator of neuronal activity. Co-overexpression of both sHSPs results in enhanced intracellular calcium activity directly associated to neuronal activity. Therefore, small chaperones are required for the formation of the correct synapse number in NMJs and also can stimulate brain activity. These results connect neural activity and chaperones, which are proteins that sense environmental changes and in consequence, link neural activity and environment during development. In particular, these two chaperones are associated to temperature changes [48, 49], environmental-stress-induced degeneration [50, 51] and lifespan [52]. Besides, maternal loading of sHSP23 determines embryonic thermal tolerance pointing to a physiological role during development [53]. All these evidences support that *sHsp* disruption during embryogenesis and development can be associated to physiological defects in adulthood, therefore Pkm-sHSPs contribution during development is proposed as a central mechanism for nervous system correct formation, function and response to environmental stress.

Supporting information

S1 Fig. Tools validation. (A-B) To validate if the antibody that we generated against sHsp26 is specific, we knocked down *sHsp26* in the posterior compartment of wing imaginal disc (*engrailed-Gal4*) and visualized the specific domain with the co-expression of GFP. (C) The quantifications of pixel intensity show that anti-sHsp26 recognizes the reduction of *sHsp26* expression caused by *UAS-sHsp26 RNAi*. Unpaired T-test Welch's correction **** p value < 0,0001. Error bars show S.D.

(TIF)

S1 Raw images.

(PDF)

Acknowledgments

We thank Professor Alberto Ferrús, Dr. F.A. Martín, María Losada, Patricia Jarabo and anonymous reviewers for critiques of the manuscript and for helpful discussions. Clemencia Cuadrado for fly stocks maintenance. We are grateful to the Vienna *Drosophila* Resource Centre, the Bloomington *Drosophila* stock Centre and the Developmental Studies Hybridoma Bank for supplying fly stocks and antibodies, and FlyBase for its wealth of information. We acknowledge the support of the Confocal Microscopy unit and Molecular Biology unit at the Cajal Institute for their help with this project. We acknowledge support of the publication fee by the CSIC Open Access Publication Support Initiative through its Unit of Information Resources for Research (URICI).

Author Contributions

Conceptualization: Elena Santana, Sergio Casas-Tintó.

Formal analysis: Elena Santana, Teresa de los Reyes, Sergio Casas-Tintó.

Funding acquisition: Sergio Casas-Tintó.

Investigation: Elena Santana, Teresa de los Reyes, Sergio Casas-Tintó.

Methodology: Elena Santana, Teresa de los Reyes, Sergio Casas-Tintó.

Project administration: Sergio Casas-Tintó.

Supervision: Sergio Casas-Tintó.

Writing – original draft: Elena Santana, Teresa de los Reyes, Sergio Casas-Tintó.

References

1. Liston C, Miller MM, Goldwater DS, Radley JJ, Rocher AB, Hof PR, et al. Stress-induced alterations in prefrontal cortical dendritic morphology predict selective impairments in perceptual attentional set-shifting. *J Neurosci*. 2006; 26(30):7870–4. Epub 2006/07/28. 26/30/7870 [pii] <https://doi.org/10.1523/JNEUROSCI.1184-06.2006> PMID: 16870732; PubMed Central PMCID: PMC6674229.
2. Bakthisaran R, Tangirala R, Rao Ch M. Small heat shock proteins: Role in cellular functions and pathology. *Biochim Biophys Acta*. 2015; 1854(4):291–319. Epub 2015/01/04. S1570-9639(14)00335-5 [pii] <https://doi.org/10.1016/j.bbapap.2014.12.019> PMID: 25556000.
3. Beere HM. "The stress of dying": the role of heat shock proteins in the regulation of apoptosis. *J Cell Sci*. 2004; 117(Pt 13):2641–51. Epub 2004/06/01. <https://doi.org/10.1242/jcs.01284> [pii]. PMID: 15169835.
4. Kamradt MC, Lu M, Werner ME, Kwan T, Chen F, Strohecker A, et al. The small heat shock protein alpha B-crystallin is a novel inhibitor of TRAIL-induced apoptosis that suppresses the activation of caspase-3. *J Biol Chem*. 2005; 280(12):11059–66. Epub 2005/01/18. M413382200 [pii] <https://doi.org/10.1074/jbc.M413382200> PMID: 15653686.
5. Wettstein G, Bellaye PS, Micheau O, Bonniaud P. Small heat shock proteins and the cytoskeleton: an essential interplay for cell integrity? *Int J Biochem Cell Biol*. 2012; 44(10):1680–6. Epub 2012/06/12. S1357-2725(12)00190-2 [pii] <https://doi.org/10.1016/j.biocel.2012.05.024> PMID: 22683760.
6. Bai F, Xi J, Higashikubo R, Andley UP. Cell kinetic status of mouse lens epithelial cells lacking alphaA- and alphaB-crystallin. *Mol Cell Biochem*. 2004; 265(1–2):115–22. Epub 2004/11/17. <https://doi.org/10.1023/b:mcbi.0000044365.48900.82> PMID: 15543941.
7. Van Montfort R, Slingsby C, Vierling E. Structure and function of the small heat shock protein/alpha-crystallin family of molecular chaperones. *Adv Protein Chem*. 2001; 59:105–56. Epub 2002/03/01. [https://doi.org/10.1016/s0065-3233\(01\)59004-x](https://doi.org/10.1016/s0065-3233(01)59004-x) PMID: 11868270.
8. Hartl FU, Bracher A, Hayer-Hartl M. Molecular chaperones in protein folding and proteostasis. *Nature*. 2011; 475(7356):324–32. Epub 2011/07/22. nature10317 [pii] <https://doi.org/10.1038/nature10317> PMID: 21776078.
9. Raut S, Mallik B, Parichha A, Amrutha V, Sahi C, Kumar V. RNAi-Mediated Reverse Genetic Screen Identified Drosophila Chaperones Regulating Eye and Neuromuscular Junction Morphology. *G3 (Bethesda)*. 2017; 7(7):2023–38. Epub 2017/05/14. g3.117.041632 [pii] <https://doi.org/10.1534/g3.117.041632> PMID: 28500055; PubMed Central PMCID: PMC5499113.
10. Jagla T, Dubinska-Magiera M, Poovathumkadavil P, Daczewska M, Jagla K. Developmental Expression and Functions of the Small Heat Shock Proteins in Drosophila. *Int J Mol Sci*. 2018; 19(11). Epub 2018/11/08. ijms19113441 [pii] <https://doi.org/10.3390/ijms19113441> PMID: 30400176; PubMed Central PMCID: PMC6274884.
11. Sun Y, MacRae TH. Small heat shock proteins: molecular structure and chaperone function. *Cell Mol Life Sci*. 2005; 62(21):2460–76. Epub 2005/09/07. <https://doi.org/10.1007/s00018-005-5190-4> PMID: 16143830.
12. Lahvic JL, Ji Y, Marin P, Zufacht JP, Springel MW, Wosen JE, et al. Small heat shock proteins are necessary for heart migration and laterality determination in zebrafish. *Dev Biol*. 2013; 384(2):166–80. Epub 2013/10/22. S0012-1606(13)00540-X [pii] <https://doi.org/10.1016/j.ydbio.2013.10.009> PMID: 24140541; PubMed Central PMCID: PMC3924900.
13. Webster JM, Darling AL, Uversky VN, Blair LJ. Small Heat Shock Proteins, Big Impact on Protein Aggregation in Neurodegenerative Disease. *Front Pharmacol*. 2019; 10:1047. Epub 2019/10/18. <https://doi.org/10.3389/fphar.2019.01047> PMID: 31619995; PubMed Central PMCID: PMC6759932.
14. Houck SA, Clark JI. Dynamic subunit exchange and the regulation of microtubule assembly by the stress response protein human alphaB crystallin. *PLoS One*. 2010; 5(7):e11795. Epub 2010/07/30. <https://doi.org/10.1371/journal.pone.0011795> PMID: 20668689; PubMed Central PMCID: PMC2909917.
15. Kriehuber T, Rattei T, Weinmaier T, Bepperling A, Haslbeck M, Buchner J. Independent evolution of the core domain and its flanking sequences in small heat shock proteins. *FASEB J*. 2010; 24(10):3633–42. Epub 2010/05/27. fj.10-156992 [pii] <https://doi.org/10.1096/fj.10-156992> PMID: 20501794.
16. Haslbeck M, Vierling E. A first line of stress defense: small heat shock proteins and their function in protein homeostasis. *J Mol Biol*. 2015; 427(7):1537–48. Epub 2015/02/15. S0022-2836(15)00081-9 [pii] <https://doi.org/10.1016/j.jmb.2015.02.002> PMID: 25681016; PubMed Central PMCID: PMC4360138.

17. Muller P, Ruckova E, Halada P, Coates PJ, Hrstka R, Lane DP, et al. C-terminal phosphorylation of Hsp70 and Hsp90 regulates alternate binding to co-chaperones CHIP and HOP to determine cellular protein folding/degradation balances. *Oncogene*. 2013; 32(25):3101–10. Epub 2012/07/25. onc2012314 [pii] <https://doi.org/10.1038/onc.2012.314> PMID: 22824801.
18. Karunanithi S, Barclay JW, Robertson RM, Brown IR, Atwood HL. Neuroprotection at Drosophila synapses conferred by prior heat shock. *J Neurosci*. 1999; 19(11):4360–9. Epub 1999/05/26. <https://doi.org/10.1523/JNEUROSCI.19-11-04360.1999> PMID: 10341239; PubMed Central PMCID: PMC6782588.
19. Kim JY, Kim JW, Yenari MA. Heat Shock Protein Signaling in Brain Ischemia and Injury. *Neurosci Lett*. 2019;134642. Epub 2019/11/24. S0304-3940(19)30745-1 [pii] <https://doi.org/10.1016/j.neulet.2019.134642> PMID: 31759081.
20. Warrick JM, Chan HY, Gray-Board GL, Chai Y, Paulson HL, Bonini NM. Suppression of polyglutamine-mediated neurodegeneration in Drosophila by the molecular chaperone HSP70. *Nat Genet*. 1999; 23(4):425–8. Epub 1999/12/02. <https://doi.org/10.1038/70532> PMID: 10581028.
21. Muchowski PJ, Wacker JL. Modulation of neurodegeneration by molecular chaperones. *Nat Rev Neurosci*. 2005; 6(1):11–22. Epub 2004/12/22. nrm1587 [pii] <https://doi.org/10.1038/nrn1587> PMID: 15611723.
22. Klose MK, Robertson RM. Stress-induced thermoprotection of neuromuscular transmission. *Integr Comp Biol*. 2004; 44(1):14–20. Epub 2004/02/01. 44/1/14 [pii] <https://doi.org/10.1093/icb/44.1.14> PMID: 21680481.
23. Morrison JH, Baxter MG. The ageing cortical synapse: hallmarks and implications for cognitive decline. *Nat Rev Neurosci*. 2012; 13(4):240–50. Epub 2012/03/08. nrm3200 [pii] <https://doi.org/10.1038/nrn3200> PMID: 22395804; PubMed Central PMCID: PMC3592200.
24. Hyer MM, Phillips LL, Neigh GN. Sex Differences in Synaptic Plasticity: Hormones and Beyond. *Front Mol Neurosci*. 2018; 11:266. Epub 2018/08/16. <https://doi.org/10.3389/fnmol.2018.00266> PMID: 30108482; PubMed Central PMCID: PMC6079238.
25. Hosoda R, Nakayama K, Kato-Negishi M, Kawahara M, Muramoto K, Kuroda Y. Thyroid hormone enhances the formation of synapses between cultured neurons of rat cerebral cortex. *Cell Mol Neurobiol*. 2003; 23(6):895–906. Epub 2004/02/18. <https://doi.org/10.1023/b:cebm.0000005318.53810.de> PMID: 14964777.
26. Bettio L, Thacker JS, Hutton C, Christie BR. Modulation of synaptic plasticity by exercise. *Int Rev Neurobiol*. 2019; 147:295–322. Epub 2019/10/15. S0074-7742(19)30048-0 [pii] <https://doi.org/10.1016/bs.irm.2019.07.002> PMID: 31607359.
27. Wishart TM, Parson SH, Gillingwater TH. Synaptic vulnerability in neurodegenerative disease. *J Neuro-pathol Exp Neurol*. 2006; 65(8):733–9. Epub 2006/08/10. <https://doi.org/10.1097/01.jnen.0000228202.35163.c4> [pii]. PMID: 16896307.
28. Gillingwater TH, Wishart TM. Mechanisms underlying synaptic vulnerability and degeneration in neurodegenerative disease. *Neuropathol Appl Neurobiol*. 2013; 39(4):320–34. Epub 2013/01/08. <https://doi.org/10.1111/nan.12014> PMID: 23289367.
29. Dickman DK, Lu Z, Meinertzhagen IA, Schwarz TL. Altered synaptic development and active zone spacing in endocytosis mutants. *Curr Biol*. 2006; 16(6):591–8. Epub 2006/03/21. S0960-9822(06)01209-7 [pii] <https://doi.org/10.1016/j.cub.2006.02.058> PMID: 16546084.
30. Jordan-Alvarez S, Santana E, Casas-Tinto S, Acebes A, Ferrus A. The equilibrium between antagonistic signaling pathways determines the number of synapses in Drosophila. *PLoS One*. 2017; 12(9):e0184238. Epub 2017/09/12. <https://doi.org/10.1371/journal.pone.0184238> [pii]. PMID: 28892511; PubMed Central PMCID: PMC5593197.
31. Atwood HL, Govind CK, Wu CF. Differential ultrastructure of synaptic terminals on ventral longitudinal abdominal muscles in Drosophila larvae. *J Neurobiol*. 1993; 24(8):1008–24. Epub 1993/08/01. <https://doi.org/10.1002/neu.480240803> PMID: 8409966.
32. Keshishian H, Broadie K, Chiba A, Bate M. The drosophila neuromuscular junction: a model system for studying synaptic development and function. *Annu Rev Neurosci*. 1996; 19:545–75. Epub 1996/01/01. <https://doi.org/10.1146/annurev.ne.19.030196.002553> PMID: 8833454.
33. Mason JM, Strobel E, Green MM. mu-2: mutator gene in Drosophila that potentiates the induction of terminal deficiencies. *Proc Natl Acad Sci U S A*. 1984; 81(19):6090–4. Epub 1984/10/01. <https://doi.org/10.1073/pnas.81.19.6090> PMID: 6435123; PubMed Central PMCID: PMC391865.
34. Marin R, Valet JP, Tanguay RM. hsp23 and hsp26 exhibit distinct spatial and temporal patterns of constitutive expression in Drosophila adults. *Dev Genet*. 1993; 14(1):69–77. Epub 1993/01/01. <https://doi.org/10.1002/dvg.1020140109> PMID: 8482013.
35. Brand AH, Perrimon N. Targeted gene expression as a means of altering cell fates and generating dominant phenotypes. *Development*. 1993; 118(2):401–15. Epub 1993/06/01. PMID: 8223268.

36. Guruharsha KG, Rual JF, Zhai B, Mintseris J, Vaidya P, Vaidya N, et al. A protein complex network of *Drosophila melanogaster*. *Cell*. 2011; 147(3):690–703. Epub 2011/11/01. <https://doi.org/10.1016/j.cell.2011.08.047> PMID: 22036573; PubMed Central PMCID: PMC3319048.
37. Parcellier A, Schmitt E, Brunet M, Hammann A, Solary E, Garrido C. Small heat shock proteins HSP27 and alphaB-crystallin: cytoprotective and oncogenic functions. *Antioxid Redox Signal*. 2005; 7(3–4):404–13. Epub 2005/02/12. <https://doi.org/10.1089/ars.2005.7.404> PMID: 15706087.
38. Weeks SD, Baranova EV, Heirbaut M, Beelen S, Shkumatov AV, Gusev NB, et al. Molecular structure and dynamics of the dimeric human small heat shock protein HSPB6. *J Struct Biol*. 2014; 185(3):342–54. Epub 2014/01/03. S1047-8477(13)00336-5 [pii] <https://doi.org/10.1016/j.jsb.2013.12.009> PMID: 24382496.
39. Baldwin AJ, Lioe H, Robinson CV, Kay LE, Benesch JL. alphaB-crystallin polydispersity is a consequence of unbiased quaternary dynamics. *J Mol Biol*. 2011; 413(2):297–309. Epub 2011/08/16. S0022-2836(11)00770-4 [pii] <https://doi.org/10.1016/j.jmb.2011.07.016> PMID: 21839090.
40. Masuyama K, Zhang Y, Rao Y, Wang JW. Mapping neural circuits with activity-dependent nuclear import of a transcription factor. *J Neurogenet*. 2012; 26(1):89–102. Epub 2012/01/13. <https://doi.org/10.3109/01677063.2011.642910> PMID: 22236090; PubMed Central PMCID: PMC3357894.
41. Lai SL, Lee T. Genetic mosaic with dual binary transcriptional systems in *Drosophila*. *Nat Neurosci*. 2006; 9(5):703–9. Epub 2006/04/04. nn1681 [pii] <https://doi.org/10.1038/nn1681> PMID: 16582903.
42. Das SC, Chen D, Callor WB, Christensen E, Coon H, Williams ME. Dii-mediated analysis of presynaptic and postsynaptic structures in human postmortem brain tissue. *J Comp Neurol*. 2019; 527(18):3087–98. Epub 2019/06/04. <https://doi.org/10.1002/cne.24722> PMID: 31152449; PubMed Central PMCID: PMC6790174.
43. Shahidullah M, Le Marchand SJ, Fei H, Zhang J, Pandey UB, Dalva MB, et al. Defects in synapse structure and function precede motor neuron degeneration in *Drosophila* models of FUS-related ALS. *J Neurosci*. 2013; 33(50):19590–8. Epub 2013/12/18. 33/50/19590 [pii] <https://doi.org/10.1523/JNEUROSCI.3396-13.2013> PMID: 24336723; PubMed Central PMCID: PMC3858628.
44. Bercier V, Hubbard JM, Fidelin K, Duroure K, Auer TO, Revenu C, et al. Dynactin1 depletion leads to neuromuscular synapse instability and functional abnormalities. *Mol Neurodegener*. 2019; 14(1):27. Epub 2019/07/12. <https://doi.org/10.1186/s13024-019-0327-3> [pii]. PMID: 31291987; PubMed Central PMCID: PMC6617949.
45. O'Connor E, Cairns G, Spendiff S, Burns D, Hettwer S, Mader A, et al. Modulation of Agrin and RhoA Pathways Ameliorates Movement Defects and Synapse Morphology in MYO9A-Depleted Zebrafish. *Cells*. 2019; 8(8). Epub 2019/08/10. cells8080848 [pii] <https://doi.org/10.3390/cells8080848> PMID: 31394789; PubMed Central PMCID: PMC6721702.
46. Takeuchi K, Gertner MJ, Zhou J, Parada LF, Bennett MV, Zukin RS. Dysregulation of synaptic plasticity precedes appearance of morphological defects in a Pten conditional knockout mouse model of autism. *Proc Natl Acad Sci U S A*. 2013; 110(12):4738–43. Epub 2013/03/15. 1222803110 [pii] <https://doi.org/10.1073/pnas.1222803110> PMID: 23487788; PubMed Central PMCID: PMC3607034.
47. Singh LR, Kruger WD. Functional rescue of mutant human cystathionine beta-synthase by manipulation of Hsp26 and Hsp70 levels in *Saccharomyces cerevisiae*. *J Biol Chem*. 2009; 284(7):4238–45. Epub 2008/12/17. M806387200 [pii] <https://doi.org/10.1074/jbc.M806387200> PMID: 19074437; PubMed Central PMCID: PMC2640983.
48. Franzmann TM, Menhorn P, Walter S, Buchner J. Activation of the chaperone Hsp26 is controlled by the rearrangement of its thermosensor domain. *Mol Cell*. 2008; 29(2):207–16. Epub 2008/02/05. S1097-2765(07)00820-9 [pii] <https://doi.org/10.1016/j.molcel.2007.11.025> PMID: 18243115.
49. Colinet H, Lee SF, Hoffmann A. Knocking down expression of Hsp22 and Hsp23 by RNA interference affects recovery from chill coma in *Drosophila melanogaster*. *J Exp Biol*. 2010; 213(Pt 24):4146–50. Epub 2010/11/30. 213/24/4146 [pii] <https://doi.org/10.1242/jeb.051003> PMID: 21112994.
50. Michaud S, Tanguay RM. Expression of the Hsp23 chaperone during *Drosophila* embryogenesis: association to distinct neural and glial lineages. *BMC Dev Biol*. 2003; 3:9. Epub 2003/11/18. <https://doi.org/10.1186/1471-213X-3-9> [pii]. PMID: 14617383; PubMed Central PMCID: PMC293469.
51. Kawasaki F, Koonce NL, Guo L, Fatima S, Qiu C, Moon MT, et al. Small heat shock proteins mediate cell-autonomous and -nonautonomous protection in a *Drosophila* model for environmental-stress-induced degeneration. *Dis Model Mech*. 2016; 9(9):953–64. Epub 2016/08/03. dmm.026385 [pii] <https://doi.org/10.1242/dmm.026385> PMID: 27483356; PubMed Central PMCID: PMC5047692.
52. Wang HD, Kazemi-Esfarjani P, Benzer S. Multiple-stress analysis for isolation of *Drosophila* longevity genes. *Proc Natl Acad Sci U S A*. 2004; 101(34):12610–5. Epub 2004/08/17. <https://doi.org/10.1073/pnas.0404648101> [pii]. PMID: 15308776; PubMed Central PMCID: PMC515105.
53. Lockwood BL, Julick CR, Montooth KL. Maternal loading of a small heat shock protein increases embryo thermal tolerance in *Drosophila melanogaster*. *J Exp Biol*. 2017; 220(Pt 23):4492–501. Epub 2017/11/04. jeb.164848 [pii] <https://doi.org/10.1242/jeb.164848> PMID: 29097593; PubMed Central PMCID: PMC5769566.